Cell

A DNA-Dependent Protease Involved in DNA-Protein Crosslink Repair

Julian Stingele,[1] Michael S. Schwarz,[1] Nicolas Bloemeke,[1] Peter G. Wolf,[1,2] and Stefan Jentsch[1,*]
[1]Department of Molecular Cell Biology, Max Planck Institute of Biochemistry, Am Klopferspitz 18, 82152 Martinsried, Germany
[2]Present address: University of Bayreuth, Universitätsstr. 30, 95540 Bayreuth, Germany
*Correspondence: jentsch@biochem.mpg.de
http://dx.doi.org/10.1016/j.cell.2014.04.053

SUMMARY

Toxic DNA-protein crosslinks (DPCs) arise by ionizing irradiation and UV light, are particularly caused by endogenously produced reactive compounds such as formaldehyde, and also occur during compromised topoisomerase action. Although nucleotide excision repair and homologous recombination contribute to cell survival upon DPCs, hardly anything is known about mechanisms that target the protein component of DPCs directly. Here, we identify the metalloprotease Wss1 as being crucial for cell survival upon exposure to formaldehyde and topoisomerase 1-dependent DNA damage. Yeast mutants lacking Wss1 accumulate DPCs and exhibit gross chromosomal rearrangements. Notably, in vitro assays indicate that substrates such as topoisomerase 1 are processed by the metalloprotease directly and in a DNA-dependent manner. Thus, our data suggest that Wss1 contributes to survival of DPC-harboring cells by acting on DPCs proteolytically. We propose that DPC proteolysis enables repair of these unique lesions via downstream canonical DNA repair pathways.

INTRODUCTION

Genome integrity and hence cell viability are constantly threatened by DNA damage, originating from exogenous and endogenous sources (Friedberg et al., 2014; Hoeijmakers, 2001). However, DNA repair and DNA damage tolerance pathways have evolved that counteract these obstacles (Friedberg et al., 2014). DNA lesions are extremely diverse in nature and range from small DNA adducts to chromosome breaks and therefore require highly specialized pathways for repair. The DNA repair pathways that deal with damages like small and bulky DNA adducts, single-strand and double-strand breaks, or DNA interstrand crosslinks have been extensively studied and are thus well understood (Li and Heyer, 2008; Lieber, 2010; Moldovan and D'Andrea, 2009; Nouspikel, 2009; Zharkov, 2008). However, the threat posed by proteins covalently crosslinked to DNA (DNA-protein crosslinks [DPCs]) has been rather neglected, with the exception of crosslinks caused by faulty topoisomerase action (Pommier et al., 2006).

Topoisomerase 1 (Top1) is an enzyme that cuts and religates one strand of double-stranded DNA in order to relax the DNA from torsional stresses, such as those that arise during replication (Pommier et al., 2006). During the normal reaction cycle of the enzyme, Top1 forms a covalent adduct of itself with DNA as a highly transient intermediate (Pommier et al., 2006). However, DNA lesions, such as abasic sites, cause a misalignment of DNA strands, which prevents religation of the DNA, resulting in a persistent trapping of Top1 cleavage complexes (Top1ccs) (Pourquier et al., 1997). In addition, Top1ccs can be reversibly induced by the compound camptothecin (CPT, derivatives are used in cancer therapy), which interferes with DNA religation by binding to the Top1-DNA interface. Previously, a Top1cc-specific repair pathway has been described, which apparently depends on partial proteasomal degradation of the Top1cc (Desai et al., 1997). The peptide remnant that remains covalently bound to DNA is subsequently removed by tyrosyl-DNA phosphodiesterase 1 (Tdp1), which catalyzes the hydrolysis of the bond between Top1's catalytic tyrosine residue and the 3′ DNA end of the nicked DNA (Pommier et al., 2006; Pouliot et al., 1999).

DPCs also arise upon exposure to agents such as ionizing radiation, UV light, and metals such as chromium and nickel and are particularly caused by reactive aldehydes such as formaldehyde (FA; CH_2O) (Barker et al., 2005). Notably, reactive aldehydes are not restricted to exogenous sources but are also byproducts of cellular processes, including amino acid metabolism and enzymatic histone demethylation at chromatin (Swenberg et al., 2011).

DPCs, if left unrepaired, inhibit transcription as well as DNA unwinding during replication and may therefore result in genome instability or even cell death (Barker et al., 2005; Fu et al., 2011; Kohn et al., 2000; Nakano et al., 2013). Studies in yeast indicated that homologous recombination (HR) and nucleotide excision repair (NER) contribute to resistance toward FA exposure (de Graaf et al., 2009). NER is thought to excise the entire DPC, but in vitro and in vivo data indicate that it cannot act on large DPCs (Baker et al., 2007; Minko et al., 2002; Nakano et al., 2007). By contrast, as suggested by studies in prokaryotes, HR apparently acts on DPCs independent of their size (Nakano et al., 2007). Notably, these canonical DNA repair pathways also act on other lesions and target specifically the DNA component of the DPC. Proteasome inhibition results in less-efficient repair of FA-induced DPCs (Baker et al., 2007; Quievryn and

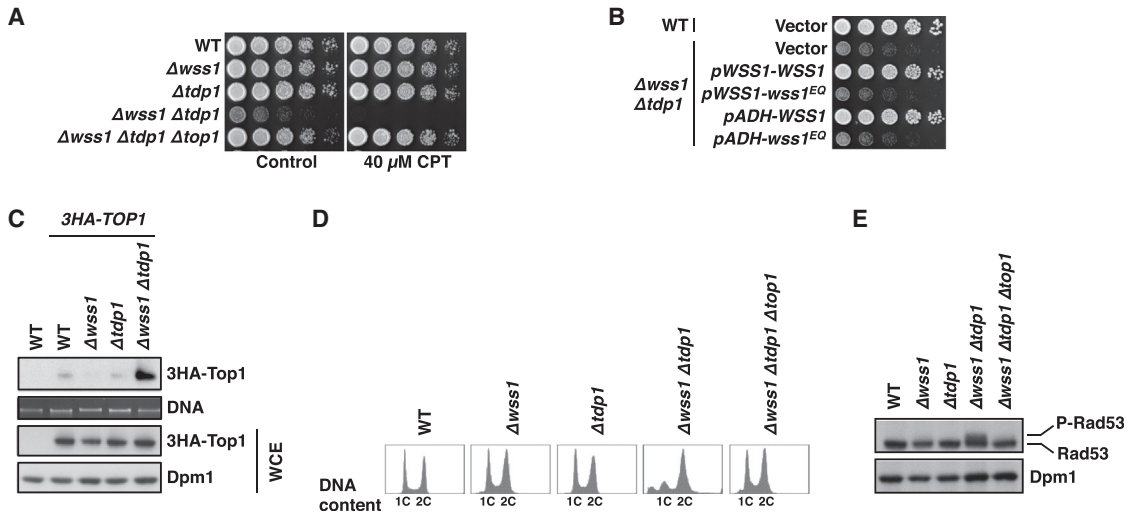

Figure 1. Wss1 Is Involved in the Processing of Top1ccs

(A) Cells lacking Wss1 and Tdp1 (*Δwss1 Δtdp1*) display severe sickness and are extremely sensitive toward CPT. The observed sickness and sensitivity are almost completely rescued in cells lacking additionally Top1. Five-fold serial dilutions of cells were spotted on YPD plates, with or without 40 μM CPT, and were incubated for 2.5 days at 30°C.

(B) The synthetic sickness of *Δwss1 Δtdp1* cells is complemented by WT Wss1, but not a mutant variant, in which the active-site residue glutamate E116 was replaced by glutamine (*wss1^{EQ}*). 3HA-tagged Wss1 variants are expressed from plasmids under control of either the endogenous promoter or the *ADH* promoter. See Figure S1D for expression levels.

(C) Cells lacking both Wss1 and Tdp1 accumulate Top1ccs. Denaturing cell extracts of 3HA-Top1-expressing cells were subjected to CsCl-gradient ultracentrifugation. The fractions containing DNA were identified (Figure S1C), concentrated, and dialyzed. DNA was quantified using agarose gel electrophoresis, followed by ethidium bromide staining. 3HA-Top1 in the DNA fraction was detected by immunoblotting after nuclease treatment using HA-specific antibodies. Whole-cell extracts (WCE) were subjected to immunoblotting as well, revealing similar levels of 3HA-Top1.

(D) The sickness of *Δwss1 Δtdp1* cells is accompanied by a G2 arrest, which depends on the presence of Top1. Samples for flow cytometry analysis of cell-cycle profiles were collected from exponentially grown cultures.

(E) Permanent DNA damage checkpoint activation indicated by Rad53 phosphorylation in *Δwss1 Δtdp1* cells. Samples were collected from exponentially grown cultures and were subjected to immunoblotting with Rad53-specific antibodies. Dpm1 levels serve as loading control.

See also Figure S1.

Zhitkovich, 2000), but the possibility that this effect might be an indirect consequence of inhibiting this major cellular proteolytic pathway cannot be excluded. Indeed, given the potential toxicity of DPCs, it seems surprising that, so far, no dedicated repair pathway that acts specifically on the protein component of DPCs, irrespective of its origin or identity, had been discovered. Here, we report the identification of the yeast metalloprotease Wss1 (weak suppressor of *smt3*) as a DNA repair factor that appears to act specifically on the protein component of DPCs. We show that Top1ccs as well as FA-induced DPCs are among Wss1's substrates and demonstrate that Wss1 enables replication of DPC-containing DNA and thus promotes genome integrity.

RESULTS

The Metalloprotease Wss1 Is Involved in Top1cc Repair

During our studies of the SUMO-protein modification system, we became interested in the yeast (*S. cerevisiae*) metalloprotease Wss1 because of its genetic and physical links to the SUMO pathway (Biggins et al., 2001; Mullen et al., 2010, 2011). However, despite these findings, little is known about the precise function of Wss1. To gain deeper insights into its cellular role, we performed an unbiased synthetic interaction screen using cells lacking Wss1 (*Δwss1*; Figure S1A available online), which identified a strong negative genetic interaction with the gene encoding Tdp1 (Figure S1B). Cells lacking Wss1 and Tdp1 (*Δwss1 Δtdp1*) suffer from severe sickness and grow extremely slowly (Figure 1A). As the crucial function of Tdp1 is linked to the repair of Top1ccs, we speculated that also Wss1 might act on Top1ccs in a pathway parallel to Tdp1. Indeed, *Δwss1 Δtdp1* cells are extremely sensitive toward the Top1cc-inducing drug CPT (Figure 1A). To test this hypothesis further, we deleted in cells lacking Wss1 and Tdp1 additionally the gene encoding Top1 (*Δwss1 Δtdp1 Δtop1*). Strikingly, the severe sickness was rescued almost entirely (Figures 1A and S1C), indicating persistent Top1ccs as the underlying cause of the observed phenotype. As Wss1 bears an amino (N)-terminal protease domain (Iyer et al., 2004), we next asked whether its catalytic activity might be required to fulfill its function. In fact, replacement of the active-site glutamate residue E116 by glutamine resulted in a variant (*wss1^{EQ}*) not capable of complementing the loss of Wss1, even when strongly overexpressed (Figures 1B and S1D). From these data, we infer that Wss1 and its proteolytic activity are crucial in cells in which Top1ccs arise and that it acts in parallel to the pathway centered around Tdp1. Yet it remained unclear whether Top1ccs are targeted directly by Wss1. We reasoned that, if Wss1 acts on the crosslinks directly, the severe

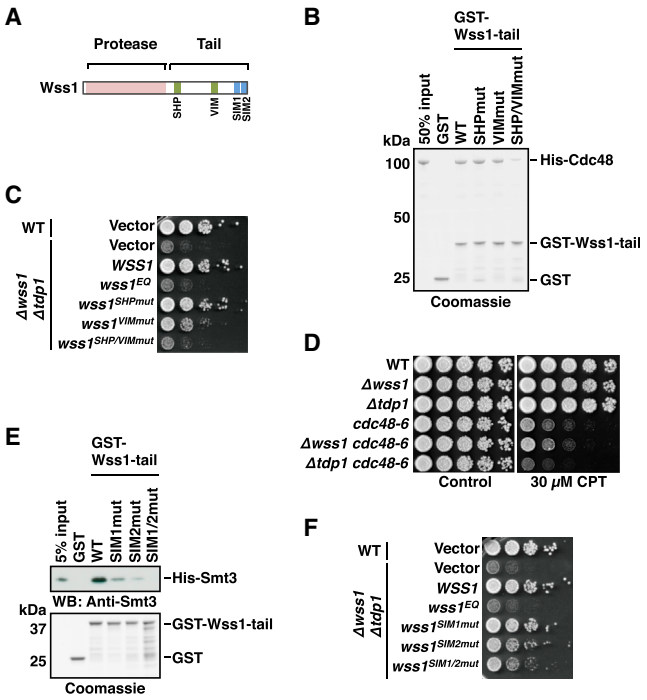

Figure 2. Wss1 Is Linked to Cdc48 and the SUMO System

(A) Schematic diagram of Wss1's domain structure.

(B) Wss1 binds Cdc48 via VIM and SHP interaction motifs. GST-tagged C-terminal tails of Wss1 or variants defective in Cdc48-interaction motifs were used in pull-down experiments with His-tagged Cdc48.

(C) Interaction with Cdc48 is critical for Wss1 function. Mutant *Δwss1 Δtdp1* cells were complemented with plasmids encoding variants of HA-tagged Wss1 under control of the endogenous promoter and spotted in 5-fold serial dilutions on YPD plates and were incubated for 2.5 days at 30°C. See Figure S2B for expression levels of Wss1 variants.

(D) Deletion of *TDP1*, but not of *WSS1*, increases the CPT sensitivity of *CDC48* mutant cells. Five-fold serial dilutions of cells were spotted on YPD plates, with or without 30 μM CPT, and were incubated for 3 days at 30°C.

(E) Wss1 binds SUMO (Smt3) via two C-terminal interaction motifs: SIM1 and SIM2. GST pull-down of GST, a GST-tagged C-terminal tail of Wss1, or variants with defective SIMs. His-Smt3 is efficiently pulled down with the C-terminal tail of Wss1, which is abolished when both SIMs are defective. Immunoblot using Smt3-specific antibodies and Coomassie blue staining are shown.

(F) Wss1 deficient in SUMO (Smt3) binding is only partially functional. *Δwss1 Δtdp1* cells were complemented with plasmid-borne 3HA-tagged Wss1 variants. Five-fold serial dilutions of cells were spotted on YPD plates and incubated for 2.5 days at 30°C. See Figure S2C for expression levels of Wss1 variants.

See also Figure S2.

sickness of *Δwss1 Δtdp1* double-mutant cells should be accompanied by an accumulation of persistent Top1ccs. To test this hypothesis, we quantified Top1ccs using a modified in vivo complex of enzyme (ICE) assay. We purified total DNA from cell extracts under harsh denaturing conditions to efficiently remove noncovalently bound proteins from DNA and isolated the DNA-containing fraction by cesium chloride gradient ultracentrifugation (Figure S1E). This fraction, expected to contain also covalently bound Top1, was then treated with nuclease and was probed for Top1 by immunoblotting. Indeed, we observed that covalent Top1 adducts accumulate strongly in cells lacking both Wss1 and Tdp1, but not in the respective single mutants (Figure 1C). Thus, Wss1 and Tdp1 act indeed in parallel and are both required for removing Top1ccs efficiently from chromatin.

Covalently trapped Top1 on DNA stalls replication fork progression, thereby inhibiting S phase completion and cell division (Regairaz et al., 2011). We thus asked whether the observed accumulation of Top1ccs in cells lacking both Wss1 and Tdp1 results in cell-cycle phenotypes. Indeed, *Δwss1 Δtdp1* cells accumulate strongly in the late-S/G2 phase of the cell cycle (Figure 1D). Intriguingly, this cell-cycle defect can be completely attributed to accumulated Top1ccs, as deletion of the gene encoding Top1 restores normal cell-cycle progression (Figure 1D). Moreover, using Rad53 phosphorylation as an indicator for DNA damage checkpoint activation, we observed that the checkpoint was indeed noticeably turned on when Top1ccs accumulate in *Δwss1 Δtdp1* cells (Figure 1E). However, an activated checkpoint is only to a lesser degree responsible for the slow growth of *Δwss1 Δtdp1* cells, as abrogation of the checkpoint (by deletion of *RAD9*) alleviates the sickness only very mildly (Figure S1F). As the observed checkpoint activation also strictly depended on the presence of Top1, we conclude that Wss1 is a new factor directly acting on Top1ccs and that it acts in parallel to Tdp1 in preventing replication stress in the presence of Top1ccs.

Wss1 Is Linked to the Cdc48 Segregase and the SUMO System

To gain further insights into Wss1 function, we addressed the role of protein-protein-interaction domains found in the carboxyl (C)-terminal tail of the protein (Figure 2A). Two sequence motifs resemble known elements involved in binding of Cdc48 (p97/VCP in mammals), a chaperone-like enzyme that binds ubiquitin- or SUMO-modified proteins and segregates them from their environment (protein complexes, membranes, or chromatin) (Bergink et al., 2013; Jentsch and Rumpf, 2007; Stolz et al., 2011). One of these motifs (VCP-interaction motif [VIM]) had been previously identified by bioinformatic prediction (Stapf et al., 2011). The other resembles a SHP box, present, e.g., in the Cdc48 cofactor Shp1 (Figures 2A and S2A) (Stolz et al., 2011). By using GST pull-down assays, we found that the tail of Wss1 and Cdc48 indeed physically interact (Figure 2B). Intriguingly, Cdc48 binding was only markedly reduced if we used a variant with replacements of crucial residues in both motifs (wss1$^{SHP/VIMmut}$, Figures 2B and S2A). To test whether Cdc48 binding is important for Wss1 function in vivo, we complemented *Δwss1 Δtdp1* cells with either wild-type (WT) Wss1 or the respective mutant variants. Intriguingly, combined elimination of both interaction motifs (*wss1*$^{SHP/VIMmut}$) resulted in a phenotype similar to a *Δwss1* deletion (Figures 2C and S2B), suggesting that Wss1 needs to associate with Cdc48 to perform its function in vivo. To strengthen this finding, we also asked whether Tdp1 becomes crucial if Cdc48 function is compromised, such as in the mutant strain *cdc48-6*. Indeed, deletion of *TDP1* increases the CPT sensitivity of *cdc48-6* cells markedly, whereas deletion of *WSS1* did not (Figure 2D).

In addition to Cdc48 interaction motifs, Wss1 bears two characteristic short SUMO-interacting motifs (SIMs) in its tail (Figures

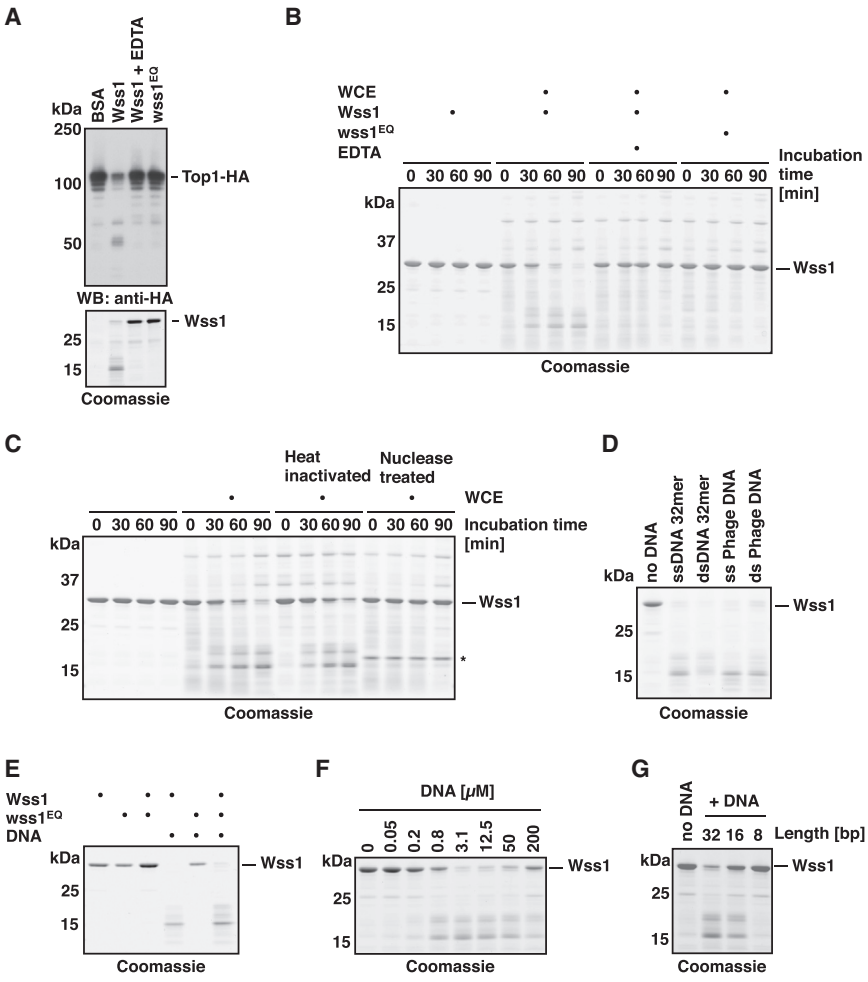

Figure 3. Wss1 Cleaves Itself in a DNA-Dependent Manner

(A) Immunopurified Top1 is cleaved by Wss1. Cleavage is inhibited by EDTA and is not detected with a catalytically inactive variant of Wss1 ($wss1^{EQ}$). Wss1 also cleaves itself, when incubated together with Top1. Top1 (immunopurified from yeast) was incubated with a control protein (BSA), recombinant Wss1, Wss1 plus 10 mM EDTA, or $wss1^{EQ}$ for 3 hr. Cleavage was monitored by SDS-PAGE followed by Coomassie blue staining or immunoblotting.

(B) Wss1 cleaves itself when incubated together with whole-cell lysate (WCE). WT Wss1 (either with or without 10 mM EDTA) or its inactive variant was incubated alone or in the presence of a WCE. The reaction was stopped by addition of Laemmli buffer at the respective time points.

(C) Induction of cleavage is inhibited by nuclease treatment of WCE. Extracts were either heat inactivated for 20 min at 80°C or treated with micrococcal nuclease (asterisk denotes nuclease) prior to addition of Wss1.

(D) DNA induces self-cleavage of Wss1. Wss1 (200 ng/μl) was incubated either alone or with several types of DNA (32 bp oligonucleotides or phage ΦX174 DNA, both single [50 ng/μl] and double stranded [100 ng/μl]) for 2 hr at 30°C prior to SDS-PAGE and Coomassie blue staining.

(E) Wss1 self-cleavage occurs in *trans*. Recombinant Wss1 or the catalytically inactive variant $wss1^{EQ}$ (both 50 ng/μl) were incubated either alone or in combination in the presence or absence of DNA (ΦX174 virion, 100 ng/μl) for 2 hr at 30°C.

(F) Recombinant Wss1 (6.6 μM) was incubated with increasing amounts of DNA (single-stranded 32 bp oligonucleotides) for 1 hr at 30°C.

(G) Recombinant Wss1 (6.6 μM) was incubated with single-stranded DNA oligonucleotides (20 μM) of different lengths for 1 hr at 30°C.

See also Figure S3.

2A and S2A) (Mullen et al., 2010). GST pull-down assays with Wss1's tail confirmed binding to His-tagged SUMO (Smt3 in yeast). Binding was strongly reduced if either of the two SIMs was rendered defective by amino acid replacements and was virtually absent if both SIMs of Wss1 were defective (Figure 2E). However, expression of Wss1 variants lacking the ability to bind SUMO (*wss1*$^{SIM1/2mut}$) partially complemented the growth phenotype of *Δwss1 Δtdp1* cells (Figures 2F and S2C), indicating that, although SUMO binding apparently contributes to the cellular function of Wss1, it is not strictly required. This finding was unexpected, as it was previously proposed that Wss1 functions as a SUMO-dependent isopeptidase (Mullen et al., 2010). Specifically, it was reported that immunopurified Wss1 has the unusual activity to cleave isopeptide-linked poly-SUMO chains, mixed ubiquitin-SUMO chains, and a linear ubiquitin-SUMO fusion protein (GST-Ubi-Smt3-V5) but scarcely polyubiquitin chains (Mullen et al., 2010). Because the proposed Wss1 activities are not obviously related to our findings, we first revisited this issue by testing the proposed isopeptidase activity using purified recombinant untagged Wss1 (Figure S2D). However, we found that the purified enzyme was unable to cleave a SUMO isopeptidase model substrate (Smt3-CHOP assay) as well as GST-ubiquitin-SUMO fusions (Figures S2E and S2F), though the enzyme was active in the experiments discussed below. Thus, together with our data that the in vivo function of Wss1 does not strictly depend on SUMO binding, we conclude that Wss1 is unlikely a SUMO-dependent isopeptidase.

Wss1 Cleaves Top1 Directly and Itself in a DNA-Dependent Manner

Prompted by this finding, we speculated that the Wss1 protease might rather act directly on Top1. To test this idea, we immunopurified Top1 from yeast cells and incubated it together with purified recombinant Wss1. Indeed, we found that Top1 is cleaved in vitro, giving rise to a number of cleavage products (Figures 3A, top, and S3A). Notably, cleavage was not observed when the metalloprotease was inactivated by addition of EDTA or when Wss1's catalytic site was defective ($wss1^{EQ}$; Figures 3A and S3A). Interestingly, we also noticed that Wss1 itself was cleaved in this assay, generating one major and some minor Wss1 fragments (Figure 3A, bottom). Wss1 cleavage was again inhibited by EDTA and did not occur when the catalytically

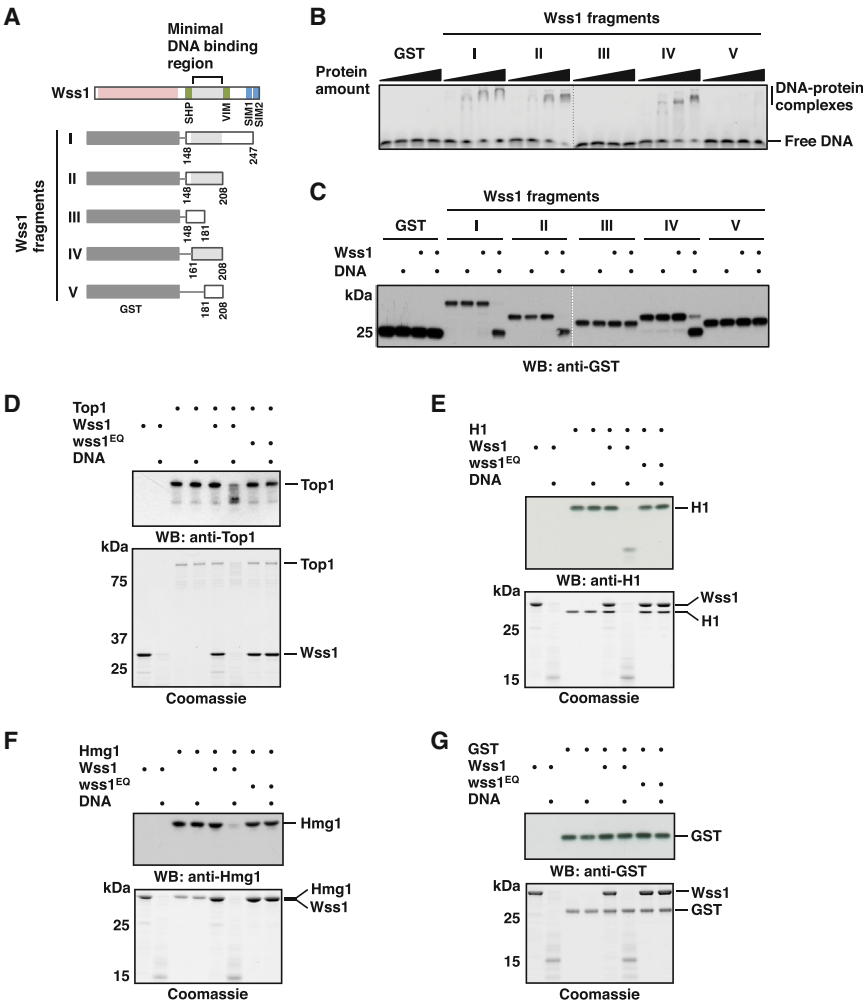

Figure 4. Wss1 Binds DNA and Targets DNA-Binding Proteins

(A) Schematic representation of Wss1 and GST-tagged C-terminal Wss1 fragments used for DNA-binding studies (light gray, minimal region required for DNA binding).

(B) The C-terminal tail of Wss1 displays DNA-binding properties. Several truncations of the tail were tested for DNA binding using EMSAs. Alexa488-labeled double-stranded DNA (21 bp) was incubated with increasing amounts of GST or GST-tagged Wss1 fragments for 20 min at room temperature prior to separation on 6% DNA retardation gels. Samples were run on two gels in parallel, as indicated by dotted line.

(C) Wss1 cleaves C-terminal fragments with DNA-binding properties in a DNA-dependent manner. GST or GST-tagged Wss1 fragments were incubated with full-length Wss1 in the absence or presence of DNA (ΦX174 virion) for 2 hr at 30°C, prior to SDS-PAGE and immunoblotting. Samples were run on two gels in parallel, as indicated by dotted line.

(D–G) Wss1 cleaves exclusively proteins with DNA-binding properties, strictly dependent on the presence of DNA. Top1, histone H1, Hmg1, or GST were incubated with Wss1 (or wss1^{EQ}), with or without adding DNA (ΦX174 virion), for 2 hr at 30°C. Cleavage was analyzed by SDS-PAGE followed either by Coomassie blue staining or by immunoblotting with protein-specific antibodies. See also Figure S4.

inactive variant of Wss1 (wss1^{EQ}) was used (Figures 3A). Surprisingly, however, Wss1 cleavage did not occur if incubated without immunopurified Top1 (Figure 3B, first left lanes), suggesting that Top1 or some factor that copurifies with Top1 induces Wss1 cleavage.

Intrigued by this finding, we asked for the nature of the activating principle. To this end, we first replaced the Top1 immunoprecipitate by a whole-cell lysate, which also induced Wss1 cleavage (Figure 3B). We could exclude Top1 as the crucial factor because extracts from yeast mutants lacking Top1 (*Δtop1*) potently activated Wss1 as well (Figure S3B). Even more surprising, heat treatment of the extract (80°C, 20 min) causing protein inactivation did not prevent activation (Figure 3C), suggesting that the activating entity is not a protein. However, as Top1 binds DNA, we speculated that perhaps DNA in the extract or DNA copurifying with Top1 was responsible for the observed Wss1 activation. Indeed, when we treated the cell lysate with nuclease, activation of Wss1 by the extract was completely abolished (Figure 3C). Importantly, simple addition of DNA of different types activated Wss1 cleavage (Figure 3D) but did not occur upon addition of nuclease-digested DNA (Figure S3C). From these findings, we thus infer that polymeric DNA, but not nucleotides, acts as an activator and that Wss1 can cleave itself. Notably, Wss1 self-cleavage can occur in *trans*, as catalytically inactive Wss1 (wss1^{EQ}) was cleaved if active Wss1 was present in the assay (Figure 3E). Moreover, Wss1 activation increased with DNA concentration yet dropped again at higher DNA levels (Figure 3F). Finally, Wss1 apparently requires a minimal DNA size for self-cleavage, as 8 mer DNA oligonucleotides failed to induce Wss1 cleavage in contrast to the potent induction by 16 and 32 mer oligonucleotides (Figure 3G). From these different lines of evidence, we infer that DNA, rather than being a typical allosteric activator, probably acts as a scaffold, bringing two naturally monomeric Wss1 molecules (Figure S3D) in proximity in these assays, thereby enabling cleavage in *trans*. The observation that high DNA concentrations are inhibitive is in fact expected from this model, as a relative high DNA concentration would reduce the probability for the association of two Wss1 molecules on the same piece of DNA.

Wss1 Targets DNA-Bound Proteins

Being a DNA-dependent protease, Wss1 is expected to bind DNA even though no known DNA-binding domain or motif was noticeable in the protein. However, when we tested fragments of Wss1's C-terminal tail as GST-fusions (Figure 4A) in an electrophoretic mobility shift assay (EMSA) using fluorescently

labeled double-stranded DNA oligonucleotides, DNA binding of Wss1 was indeed detectable and could be mapped to a 48 amino acid long region within Wss1's C-terminal tail (Figures 4A and 4B). As the aforementioned Cdc48- and SUMO-binding regions are in relative close proximity to the region responsible for DNA binding, we tested whether alterations in these motifs interfere with the DNA-dependent activity of Wss1. However, Wss1 variants deficient in Cdc48 or SUMO binding underwent self-cleavage, with kinetics indistinguishable from WT enzyme, indicating that catalytic activity and DNA binding property are unaffected by these alterations (Figure S4A).

Because Wss1 seems capable of cleaving another Wss1 molecule if they colocalize on the same DNA molecule, we expected that Wss1 is also able to cleave DNA-binding-competent fragments of Wss1 in the presence of DNA. Indeed, not GST alone, but only GST-fusions with Wss1 fragments capable of DNA binding, were cleaved by Wss1 in vitro and, remarkably, only when DNA was present (Figure 4C). Judging from this result, we hypothesized that Wss1 may generally act specifically on DNA-bound proteins. Initially focusing on Top1, we used commercially available purified human Top1 (functionally equivalent to yeast Top1 [Bjornsti et al., 1989]) and incubated the protein with Wss1 or its protease-deficient variant in the absence or presence of DNA. Indeed, Top1 was cleaved by Wss1 in this assay and again in a strictly DNA-dependent manner (Figure 4D). Analyzing the specificity of Wss1 further, we also tested cleavage of various other proteins in a similar assay. Remarkably, Wss1 was also able to cleave in a DNA-dependent manner the DNA-binding proteins histone H1 and the high mobility group protein Hmg1. By contrast, proteins with no DNA-binding properties, like GST, BSA, or the aforementioned isopeptidase substrate GST-Smt3-Ubi-V5 fusion, were not cleaved by the enzyme even in the presence of DNA (Figures 4D–4G, S4B, and S4C). Taken together with the data on Wss1 self-cleavage, these findings strongly suggest that the Wss1 protease only acts on DNA-binding proteins because DNA is needed to bring the protease and substrates together to enable proteolysis. The apparent in vitro promiscuity of Wss1 by acting on a variety of unrelated DNA-binding proteins is striking and suggested to us that Wss1 might not act exclusively on Top1ccs also in vivo.

Wss1 Is Crucial for Cell Survival upon Induction of DPCs by Formaldehyde

Intriguing candidates for additional Wss1 substrates are, e.g., chemically induced covalent DPCs, such as those that arise by exposure of chromatin to formaldehyde (FA) (Swenberg et al., 2011). To explore a potential role of Wss1 in general DPC repair, we tested yeast strains lacking Wss1 (*Δwss1*) for survival upon FA exposure. Indeed, *Δwss1* cells were hypersensitive to a short FA pulse compared to WT cells (Figure 5A). As two canonical repair pathways, NER and recombination, are known to contribute to tolerance toward FA-induced DNA damage, we asked whether Wss1 acts within one of these pathways. To this end, we compared the FA sensitivity of strains deficient in NER (*Δrad4*), recombination (*Δrad52*), or both (*Δrad4 Δrad52*) with the respective strains additionally lacking Wss1. Indeed, absence of Wss1 enhanced the FA sensitivity of the mutants yet seemingly more of the cells lacking recombination (Figure 5A). Notably, experiments measuring the FA sensitivity of *Δwss1 Δrad52* mutants complemented by different Wss1 mutant variants ($wss1^{EQ}$, $wss1^{SHP/VIMmut}$, $wss1^{SIM1/2mut}$) indicated that the proteolytic activity, as well as Cdc48 binding, are crucial for Wss1-mediated tolerance toward FA exposure, whereas SUMO binding is less important (Figures 5B and S5A). Based on these genetic data, we thus conclude that the Wss1 protease plays a critical role in FA tolerance, in addition to canonical DNA repair pathways that act on damaged DNA.

Next, we used a protocol employing protein precipitation by SDS and KCl (see Experimental Procedures), which quantifies the amount of genomic DNA coprecipitating with cellular protein as a measure of DPCs. We induced DPCs in WT and mutant strains by a short pulse of FA and followed DPC induction and repair over a period of 4 hr. Surprisingly, mutants deficient in Wss1 (*Δwss1*), Rad52 (*Δrad52*), or both (*Δwss1 Δrad52*) recovered from FA treatment virtually like WT cells, as judged from the decline of DPCs over time (Figure 5C). By contrast, mutants lacking NER retained most DPCs, suggesting defects in DPC repair. This was unexpected given that *Δwss1 Δrad52* cells are more sensitive than *Δrad4* cells (Figure 5A). On the other hand, this scenario appears to be conserved, as also in bacteria recombination provides more FA tolerance, yet removal of FA-induced DPCs seems to depend mainly on NER (Nakano et al., 2007). A straightforward interpretation of this finding is that Wss1 and recombination are not involved in the repair of the bulk of DPCs but, rather, on DPCs that are particularly toxic.

We hypothesized that NER removes most DPCs prior to replication, but those DPCs left unrepaired by NER will threaten replication in S phase and are normally repaired by Wss1 or recombination. A prediction of this model is that cells deficient in Wss1 or recombination will exhibit defects in S phase progression upon FA treatment. We tested this hypothesis by following the respective fraction of cells in different cell-cycle stages over time upon FA treatment (Figures 5D and S5B). We observed that the initial response to FA in WT cells is characterized by a drop in the S phase population accompanied by a reciprocal increase of cells in G1, a population shift that reverses over time. Notably, the overall response is similar for cells lacking NER (*Δrad4*) yet is significantly delayed, probably because the load of accumulating DPCs becomes problematic for these cells. By contrast, cells lacking Wss1 or Rad52 display initially a similar behavior to WT cells but severely accumulate cells with a G2-like DNA content upon prolonged FA exposure (Figures 5D and S5B). We thus infer from these data that DPCs that have escaped NER are compromising S phase completion and become highly problematic if either Wss1 or recombination are missing. The particularly high FA sensitivity of specifically *Δwss1 Δrad52* double mutants further indicates that Wss1 and recombination act in parallel and are partially redundant DPC tolerance pathways.

Wss1 Enables Translesion Synthesis of DPC-Containing Templates and Inhibits Gross Chromosomal Rearrangements

Another indication that Wss1 and recombination act in parallel is the reported finding that cells lacking Wss1 display increased numbers of Rad52-positive repair foci, indicative of active recombination (Alvaro et al., 2007). To investigate whether loss

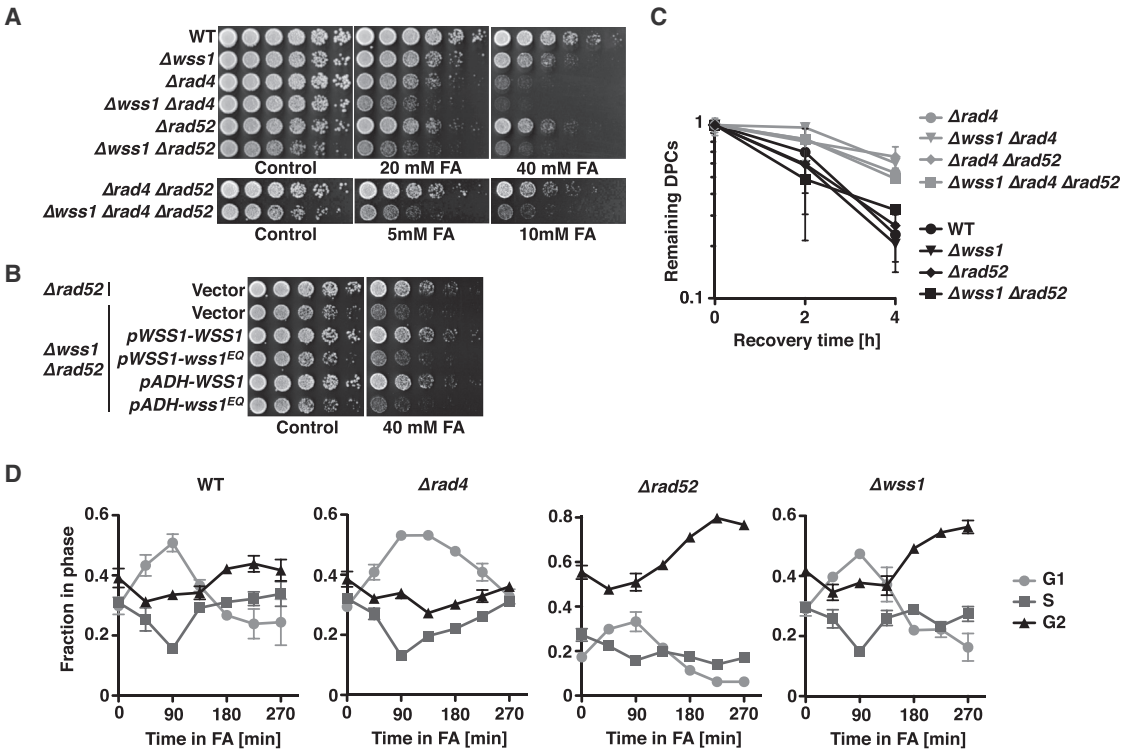

Figure 5. Wss1 Is Involved in Tolerating FA-Induced DPCs

(A) Cells lacking Wss1 (*Δwss1*), NER (*Δrad4*), or recombination (*Δrad52*) are sensitive to FA exposure. Logarithmic cultures were treated with FA for 15 min, followed by two wash steps and spotting on YPD plates. Plates were scanned after 2.5 days at 30°C.

(B) The catalytic activity of Wss1 is required for tolerating FA-induced DPCs. Cells lacking Wss1 and recombination (*Δrad52 Δwss1*) were complemented with either 3HA-tagged WT or catalytically inactive Wss1 and were tested for FA hypersensitivity. Wss1 variants are expressed from plasmids under control of either the endogenous promoter or the *ADH* promoter.

(C) NER-deficient cells (*Δrad4*) display a delay in bulk DPC removal. Mutants lacking Wss1 (*Δwss1*), NER (*Δrad4*), recombination (*Δrad52*), or double and triple mutants were subjected to a 15 min FA pulse (10 mM), followed by recovery in drug-free media. DPCs were quantified using an SDS/KCl precipitation assay. DPC levels were normalized to the 0 hr time point. Relative DPC amounts are depicted on a log 10 scale as mean ± SD of two to four independent experiments.

(D) Cells lacking either Wss1 or recombination (*Δrad52*) arrest in the G2 phase of the cell cycle when cultivated in the presence of FA. FA was added to exponentially growing cultures to a final concentration of 0.75 mM. Samples were taken every 45 min for analysis of cell-cycle profiles by flow cytometry. Quantification of cell-cycle phase distributions is shown as mean ± SD of two independent experiments.

See also Figure S5.

of Wss1 channels repair into the recombination pathway (hence increasing foci), we investigated spontaneous and FA-induced recombination rates. By measuring recombination between two nonfunctional *HIS1* hetero-alleles (located on different chromosomes), we found that recombination levels are indeed elevated in *Δwss1* cells, which was even more pronounced upon FA treatment (Figure 6A). From this finding, we thus infer that alternative DPC repair by recombination becomes particularly prominent when DPC processing by Wss1 is absent.

The downside of repair by mechanisms that rely on recombination is the risk of genome rearrangements (Mieczkowski et al., 2006). Intriguingly, elevated levels of gross chromosomal rearrangements (GCRs) have indeed been reported for cells lacking Wss1 (Kanellis et al., 2007). We excluded Top1ccs as an underlying cause, as GCR rates were independent of the presence of Top1 (Figure S6A). However, analogous to recombination between hetero-alleles (Figure 6A), GCR frequencies are strongly increased by FA in *Δwss1* strains compared to WT cells (Figure 6B). Because GCRs are thought to be caused primarily by replication fork-blocking lesions (Lambert et al., 2005) and replication progression is particularly sensitive to DPCs (Figure 5D), we assumed that Wss1 might be important for postreplicative repair (PRR). PRR becomes activated upon stalled replication, leading to either poly- or monoubiquitylation of PCNA, thereby triggering different PRR pathways (Hoege et al., 2002). Monoubiquitylation of PCNA promotes recruitment of translesion polymerases that are able to replicate across some types of lesions; however, they can incorporate the wrong nucleotides, thereby causing mutagenesis (Sale, 2013). Interestingly, FA exposure has been reported to induce mutagenesis by error-prone translesion synthesis (TLS) (Grogan and Jinks-Robertson, 2012), and we thus asked whether this observation is linked to Wss1. By measuring mutagenesis rates at the *CAN1* locus, we confirmed that FA induces mutagenesis in this assay. Astonishingly, mutagenesis was indeed largely dependent of the presence of Wss1 in cells (Figure 6C). However,

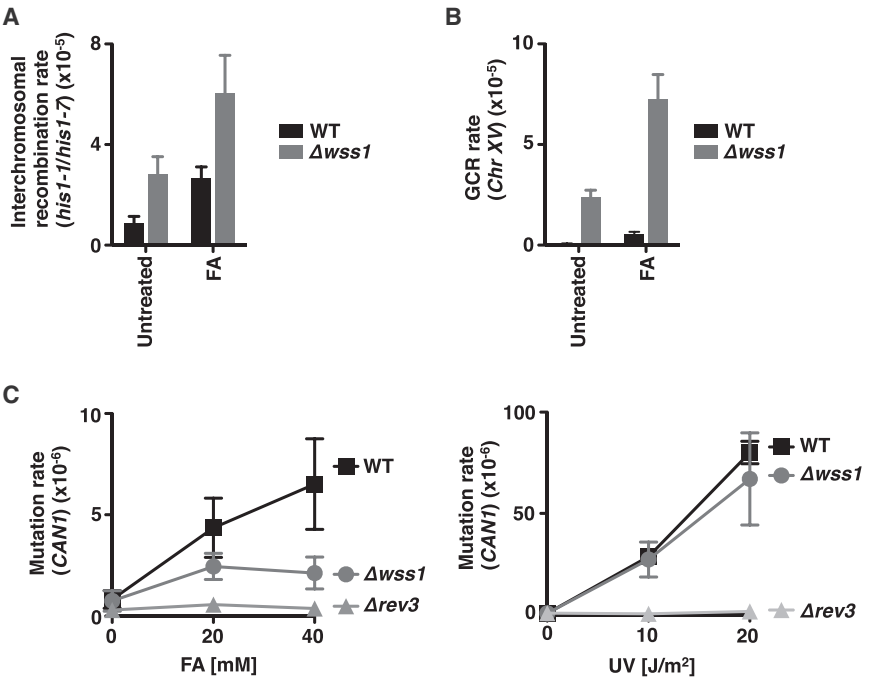

Figure 6. Wss1-Dependent DPC Processing Directs Repair Pathway Choice

(A) Interchromosomal recombination rates are higher in cells lacking Wss1 (as measured in *his1-1/his1-7* diploids), which is further increased upon FA (1 mM) treatment. Mean values of three independent fluctuation tests are shown. Error bars indicate standard deviations.

(B) Cells lacking Wss1 suffer from genomic instability, which is strongly increased upon induction of DPCs by FA (1 mM). GCR rates were determined by measuring the loss of a *CAN1-URA3* cassette inserted into the subtelomeric region of *ChrXV*. GCR rates are depicted as mean values of two to four independent fluctuation tests as mean ± SD.

(C) FA-induced mutagenesis is reduced in cells lacking Wss1 (left) yet is unchanged when induced by UV light (right). Forward mutagenesis rates were determined at the *CAN1* locus. Mutagenesis rates are depicted as mean ± SD of three to seven independent experiments.

See also Figure S6.

this effect was apparently specific for FA-induced damage, as UV light exposure induced mutagenesis irrespective of the presence of Wss1. By contrast, cells lacking the TLS polymerase Rev3 are deficient in both FA- and UV-induced mutagenesis (Figure 6C) (Grogan and Jinks-Robertson, 2012). Notably, deletion of the gene encoding Rev3 resulted in no further increase in FA sensitivity of strains lacking Wss1 or Wss1 and NER, further indicating that Wss1 and TLS collaborate in DPC repair (Figure S6B). Taken together, Wss1 is functionally connected to canonical DNA repair pathways; whereas on the one hand Wss1 suppresses DPC repair by recombination, thereby reducing the risk of GCRs, on the other hand, it facilitates replication via TLS, most likely by acting on DPCs proteolytically.

DISCUSSION

DPCs are life-threatening forms of DNA damage, as they strongly interfere with DNA transactions such as transcription and, in particular, DNA replication. DPCs arise by two types of processes, which we here designate as enzymatic and nonenzymatic. Enzymatic DPCs occur by trapping of a normally transient covalent protein-DNA intermediate during an enzymatic reaction cycle. Examples for such enzymes are topoisomerases and its relatives (Chen et al., 2013; Pommier et al., 2006). By contrast, nonenzymatic DPCs arise through chemical reactions caused by diverse exogenous or endogenous sources but, in particular, upon exposure to reactive aldehydes like formaldehyde (FA). The potential threat caused specifically by endogenous FA became vividly apparent with the discovery of histone demethylases, which release FA as a byproduct of their reaction directly at chromatin (Kooistra and Helin, 2012). Similarly, also the removal of methyl groups from DNA by AlkB-type repair enzymes generates FA in immediate vicinity to DNA and its associated proteins (Trewick et al., 2002). The drastic consequences of endogenously produced aldehydes became evident by the observation that mice lacking aldehyde-detoxifying enzymes develop anemia and leukemia when functional DNA repair (fanconi anemia pathway) is additionally missing (Garaycoechea et al., 2012; Langevin et al., 2011; Rosado et al., 2011). Notably, FA is generally tumorigenic, and exposure can, e.g., cause nasopharyngeal cancer and squamous cell carcinomas in mammals (Swenberg et al., 2011).

The DNA-dependent metalloprotease Wss1 described here is the first example of a DNA repair enzyme that appears to act specifically on the protein components of DPCs, regardless of their nature. Thus, Wss1 needs to display broad substrate specificity to process a whole spectrum of different DPCs. Notably, by using recombinant Wss1 and various substrates, we found no evidence (Figures S2E, S2F, and S4C) for a previously reported SUMO-dependent isopeptidase activity of Wss1 (Mullen et al., 2010). In fact, as pointed out before (Su and Hochstrasser, 2010), the Wss1 preparation used for the reported assays was only partially purified (Mullen et al., 2010), suggesting that the alleged activity (which could not be inhibited by EDTA) might have derived from an impurity in the enzyme preparation.

By contrast, we found that EDTA inhibits purified recombinant Wss1, as expected for a metalloprotease, and that it uniquely requires DNA for activity and selectively acts on DNA-binding proteins. However, given that Wss1 in isolation is promiscuous, as it cleaves in vitro every DNA-binding protein tested in a DNA-dependent manner, control mechanisms must exist that restrain its protease activity in vivo. Analogous to other repair enzymes, a plausible way to curb Wss1 activity is by targeting the protease preferentially to damaged DNA sites. Evidence that targeting might be linked to SUMOylation comes from the finding that Wss1 possesses SIMs, which, albeit not essential for Wss1

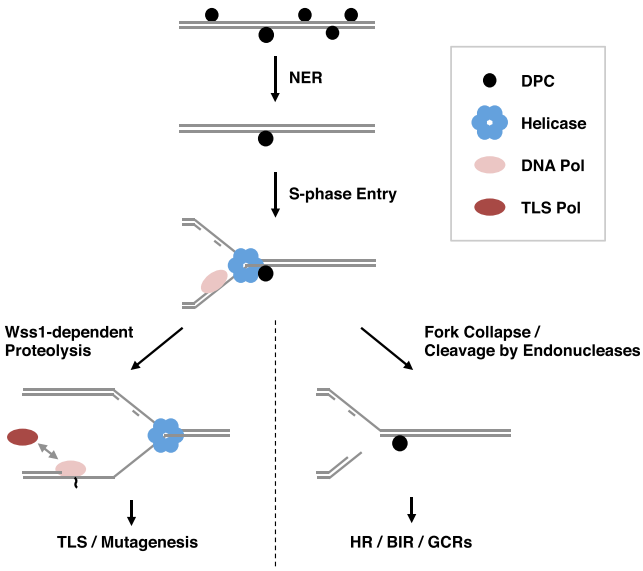

Figure 7. Hypothetical Model of DPC Repair

The bulk of DPCs are repaired by NER, but DPCs that escaped repair are expected to stall replicative helicases during S phase. Helicase stalling might be relieved by Wss1-dependent DPC processing (left). However, replicative polymerases are probably unable to replicate past the remaining lesion (proteolytic fragment remnant covalently bound to DNA), causing an uncoupling of DNA unwinding and DNA synthesis and resulting in an enlargement of single-stranded DNA. Accumulation of single-stranded DNA, in turn, promotes PCNA monoubiquitylation and subsequent recruitment of TLS polymerases. Because TLS polymerases are able to synthesize past the lesion yet potentially by misincorporation of nucleotides, mutagenesis can occur. Conversely, if a DPC is left unprocessed (right), the permanently stalled replication fork might be subjected to cleavage by endonucleases, resulting in a single-ended double-strand break. This situation may trigger recombination-dependent repair, e.g., by break-induced replication (BIR), though with the risk of genomic rearrangements (GCRs).

function, stimulate Wss1 in vivo. Because trapped Top1 (Mao et al., 2000) as well as many different DNA repair proteins accumulating at damaged DNA sites become strongly SUMOylated by DNA-bound SUMO ligases (Jentsch and Psakhye, 2013; Psakhye and Jentsch, 2012), it seems plausible that DPCs other than Top1ccs are substrates for SUMOylation as well. We thus assume that the observed supporting role of Wss1's SIMs in vivo (Figures 2F and S5A) is linked to an enhanced recruitment of Wss1 to Top1ccs and other DPCs.

Another intriguing feature of Wss1 is that it requires binding to Cdc48 for its cellular function. However, because Cdc48 is not required for Wss1 activity in vitro, Cdc48 must play other roles than supporting catalysis. Because Cdc48 and some of its cofactors also bind SUMO (Bergink et al., 2013; Nie et al., 2012), Cdc48 might assist in targeting Wss1 to SUMOylated damage sites. Moreover, given the prominent role of Cdc48 in proteasomal degradation (Jentsch and Rumpf, 2007) and its ability to dislodge proteins from chromatin (Dantuma and Hoppe, 2012), Cdc48 might directly act on the proteolytic remnants of DPCs generated by Wss1. In this model, Cdc48 might extract proteolytic fragments and deliver them depending on their size either to proteasomes or to other cellular peptidases. Alternatively, the chaperone-like activity of Cdc48 might be used to prepare DPCs for Wss1 action.

NER and recombination were previously thought to be sufficient for DPC repair (de Graaf et al., 2009). However, our discovery of Wss1 as a protease that apparently targets specifically the protein components of DPCs significantly shifts this paradigm. Based on our biochemical and genetic findings, the following model for DPC repair, albeit in part hypothetical, seems plausible (Figure 7). Our data and findings obtained previously (Nakano et al., 2007) suggest that the bulk of DPCs are, in fact, removed by NER, which excises the entire DPC, employing specific endonucleases. However, depending on the DPC load, a certain fraction of DPCs will escape repair and will remain present in DNA until S phase. Indeed, our genetic data suggest that these persisting DPCs are particularly toxic during replication, most notably when Wss1 or recombinational repair is compromised. Due to their bulkiness, DPCs are likely to already block unwinding by the replicative helicases, but this early stalling of replication might be released by the action of Wss1. However, because the Wss1 protease is unlikely to remove the crosslinked protein entirely, at least a small protein fragment will most certainly remain on DNA. The covalently bound remnants are likely to block the next step of replication: DNA synthesis conducted by replicative DNA polymerases (Figure 7, left). Uncoupling of DNA unwinding and synthesis causes an accumulation of single-stranded DNA at the replication fork, which in turn triggers PCNA ubiquitylation, leading to a recruitment of TLS polymerases. TLS polymerases are capable of synthesizing across DNA lesions yet with the risk of incorporating wrong nucleotides, thus resulting in mutagenesis. Indeed, in strong support of this model, we found that, when replication stalling is caused by DPCs, Wss1 activity is crucial for DNA replication by TLS polymerases, as inferred from the decreased FA-induced mutagenesis in *Δwss1* cells.

Conversely, in cells in which Wss1 is defective or overloaded, forks stalled at DPCs may be prone to cleavage by endonucleases, resulting in a single-ended DNA double-strand break (Figure 7, right) (Regairaz et al., 2011), which will likely result in recombinational repair by mechanisms such as break-induced replication. Our findings of especially high levels of FA-induced recombination and GCRs in the absence of Wss1 are precisely in line with this model. Notably, Wss1- and recombination-dependent mechanisms will not result in complete repair as, respectively, either a fragment or the entire DPC will remain on DNA. This might explain why no defect in DPC removal in SDS/KCl precipitation assays in cells lacking Wss1 or recombination was observed (Figure 5C).

As the action of a DPC-targeted protease is highly beneficial to cells because it promotes cell-cycle progression and genome stability in the face of DPCs, similar mechanisms are expected to operate in higher eukaryotes as well. No clear ortholog of Wss1 appears to exist in higher eukaryotes, but as pointed out previously (Mosbech et al., 2012), Wss1 might be a member of the SprT protease family whose representative in higher eukaryotes is Dvc1/Spartan. Indeed, Dvc1/Spartan displays a strikingly similar domain organization with an N-terminal metalloprotease domain and a tail harboring a Cdc48/p97 interaction module and, instead of a SIM, a ubiquitin-binding domain. Unfortunately,

the precise role of Dvc1/Spartan remains highly controversial despite recent efforts (Centore et al., 2012; Davis et al., 2012; Ghosal et al., 2012; Juhasz et al., 2012; Kim et al., 2013; Machida et al., 2012; Mosbech et al., 2012; Vaz et al., 2013). Some studies suggested that Dvc1/Spartan plays a role in conjunction with Cdc48/p97 in removal of Polη from chromatin, but the significance of Dvc1/Spartan's protease domain remained unsolved (Davis et al., 2012; Mosbech et al., 2012). Although Dvc1/Spartan may target other proteins as well and functions perhaps partially nonenzymatically, based on its domain organization and its role at the replication fork, Dvc1/Spartan remains a reasonable candidate for a Wss1-like DPC-processing enzyme and deserves further studies. At any rate, the discovery of a protease that acts in addition to canonical DNA repair pathways in detoxifying DPCs brings renewed attention to DPC repair and its importance for genome integrity.

EXPERIMENTAL PROCEDURES

Yeast Strains

Yeast (*S. cerevisiae*) strains used in this study are listed in Table S1.

Biochemical and Molecular Biology Techniques

Biochemical and molecular biology techniques used in this study are standard procedures. Detailed protocols of individual methods are described in the Extended Experimental Procedures.

Wss1 Cleavage Induction by DNA

Cleavage assays were typically performed in 10 μl reactions, containing 1 μl Wss1 (2 mg/ml) and 1 μl DNA. Several types of DNAs were used for induction of cleavage: single-stranded viral DNA (ΦX174 virion, NEB); double-stranded viral DNA (ΦX174 RF I, NEB); 32, 16, and 8 bp oligonucleotides single and double stranded.

Wss1 Substrate Cleavage Assays

Cleavage assays were typically performed in 15 μl reaction volumes, containing 2 μl substrate (0.5 mg/ml), 1 μl Wss1 (2 mg/ml), and 1 μl DNA (ΦX174 virion, 1 mg/ml). Reactions were incubated at 30°C for 2 hr if not indicated otherwise and were stopped by addition of 2× Laemmli buffer. Cleavage was monitored by SDS-PAGE, followed by either Coomassie blue staining or western blotting with substrate-specific antibodies.

DNA-Binding Assays

For analysis of DNA binding, electrophoretic mobility shift assays (EMSAs) were used. Different concentrations of the respective proteins (0.16, 0.8, 4, and 10 μM) were incubated together with fluorescently labeled double-stranded oligonucleotides (0.1 μM), followed by separation DNA retardation gels and visualization.

Cell-Cycle Analysis

For flow cytometry analysis, 1×10^7–2×10^7 cells were harvested by centrifugation and were resuspended in 70% ethanol, 50 mM Tris (pH 7.8). Next, cells were treated with RNase A and Proteinase K, followed by staining with SYTOX Green nucleic acid stain (Life Technologies) and analysis by flow cytometry.

GCR, Mutagenesis, and Recombination Assays

GCR rates were determined using fluctuation analysis. In brief, cultures (eight parallel cultures per strain) were grown overnight at 30°C. Cultures were diluted 1:20,000 in either YPD or in YPD containing 1 mM FA. Cultures were incubated for 3 days at 30°C under constant shaking. Cultures were diluted and plated on SC or SC-Arg+Can+5′-FOA plates, followed by incubation at 30°C for 3 days. GCR rates were determined using a maximum likelihood approach. Similarly, interchromosomal recombination rates were determined in diploid cells between the hetero-alleles *his1-1* and *his1-7*. FA-induced recombination rates were assayed by adding 1 mM FA (Pierce) to the growth media. Damage-induced mutagenesis was assessed at the *CAN1* locus. For measuring FA-induced mutagenesis, overnight cultures were washed once with PBS, resuspended in PBS containing FA (Sigma-Aldrich), and incubated for 15 min. After two wash steps with PBS, appropriate dilutions of cells were plated on SC or SC-Arg+Can plates and incubated for 3 days at 30°C. For UV-light-induced mutagenesis rates, overnight cultures were directly plated on SC or SC-Arg+Can plates and irradiated in an irradiation chamber. UV-light-treated cells were incubated in the dark for 3 days at 30°C. Mutation rates were calculated as the ratio between canavanine-resistant colonies to the total number of surviving cells. Each plating step was performed in triplicates.

Detection of Top1ccs

Top1ccs were detected using a modified ICE assay. In brief (see Extended Experimental Procedures for details), lysates of 3HA-Top1-expressing cells prepared under denaturing conditions were subjected to cesium chloride gradient centrifugation, which results in migration of the DNA into the bottom fractions, whereas proteins remain at the top of the gradient. Top1 covalently linked to DNA migrates together with DNA into the bottom fraction. The DNA-containing fractions were identified, pooled, concentrated, and digested with nuclease. Top1 present in the DNA fractions was visualized by immunoblotting.

Detection of FA-induced DPCs

FA-induced DPCs were detected by SDS/KCl precipitation assays. In brief (see Extended Experimental Procedures for details), cells were treated with zymolase prior to cell lysis with SDS. Cellular proteins were precipitated together with crosslinked DNA by addition of KCl, whereas soluble DNA remained in the supernatant. The precipitate was washed three times, prior to digestion of proteins and quantification of DNA on agarose gels stained with SYBR Gold (Life Technologies). The amount of DPCs was calculated as the ratio of DNA in the protein precipitate to the amount of total DNA (soluble and insoluble).

SUPPLEMENTAL INFORMATION

Supplemental Information includes Extended Experimental Procedures, six figures, and one table and can be found with this article online at http://dx.doi.org/10.1016/j.cell.2014.04.053.

AUTHOR CONTRIBUTIONS

J.S. and S.J. designed the study, analyzed the data, and wrote the paper. J.S., M.S.S., N.B., and P.G.W. conducted the experiments.

ACKNOWLEDGMENTS

We thank A. Strasser for technical assistance, J. Rech for help with robot-based techniques, the MPIB Microchemistry Core Facility for help with protein purification, and S. Bergink, M. Kern, C. Lademann, B. Pfander, I. Psakhye, and J. Renkawitz for discussions. S.J. is supported by the Max Planck Society, Deutsche Forschungsgemeinschaft, Center for Integrated Protein Science Munich, RUBICON EU Network of Excellence, ERC Advanced Grant, and the Louis-Jeantet Foundation.

Received: January 23, 2014
Revised: March 28, 2014
Accepted: April 21, 2014
Published: July 3, 2014

REFERENCES

Alvaro, D., Lisby, M., and Rothstein, R. (2007). Genome-wide analysis of Rad52 foci reveals diverse mechanisms impacting recombination. PLoS Genet. *3*, e228.

Baker, D.J., Wuenschell, G., Xia, L., Termini, J., Bates, S.E., Riggs, A.D., and O'Connor, T.R. (2007). Nucleotide excision repair eliminates unique DNA-protein cross-links from mammalian cells. J. Biol. Chem. *282*, 22592–22604.

Barker, S., Weinfeld, M., and Murray, D. (2005). DNA-protein crosslinks: their induction, repair, and biological consequences. Mutat. Res. *589*, 111–135.

Bergink, S., Ammon, T., Kern, M., Schermelleh, L., Leonhardt, H., and Jentsch, S. (2013). Role of Cdc48/p97 as a SUMO-targeted segregase curbing Rad51-Rad52 interaction. Nat. Cell Biol. *15*, 526–532.

Biggins, S., Bhalla, N., Chang, A., Smith, D.L., and Murray, A.W. (2001). Genes involved in sister chromatid separation and segregation in the budding yeast Saccharomyces cerevisiae. Genetics *159*, 453–470.

Bjornsti, M.A., Benedetti, P., Viglianti, G.A., and Wang, J.C. (1989). Expression of human DNA topoisomerase I in yeast cells lacking yeast DNA topoisomerase I: restoration of sensitivity of the cells to the antitumor drug camptothecin. Cancer Res. *49*, 6318–6323.

Centore, R.C., Yazinski, S.A., Tse, A., and Zou, L. (2012). Spartan/C1orf124, a reader of PCNA ubiquitylation and a regulator of UV-induced DNA damage response. Mol. Cell *46*, 625–635.

Chen, S.H., Chan, N.-L., and Hsieh, T.S. (2013). New mechanistic and functional insights into DNA topoisomerases. Annu. Rev. Biochem. *82*, 139–170.

Dantuma, N.P., and Hoppe, T. (2012). Growing sphere of influence: Cdc48/p97 orchestrates ubiquitin-dependent extraction from chromatin. Trends Cell Biol. *22*, 483–491.

Davis, E.J., Lachaud, C., Appleton, P., Macartney, T.J., Näthke, I., and Rouse, J. (2012). DVC1 (C1orf124) recruits the p97 protein segregase to sites of DNA damage. Nat. Struct. Mol. Biol. *19*, 1093–1100.

de Graaf, B., Clore, A., and McCullough, A.K. (2009). Cellular pathways for DNA repair and damage tolerance of formaldehyde-induced DNA-protein crosslinks. DNA Repair (Amst.) *8*, 1207–1214.

Desai, S.D., Liu, L.F., Vazquez-Abad, D., and D'Arpa, P. (1997). Ubiquitin-dependent destruction of topoisomerase I is stimulated by the antitumor drug camptothecin. J. Biol. Chem. *272*, 24159–24164.

Friedberg, E.C., Elledge, S.J., Lehmann, A.R., Lindahl, T., and Muzi-Falconi, M. (2014). DNA Repair, Mutagenesis, and Other Responses to DNA Damage (New York: Cold Spring Harbor Laboratory Press).

Fu, Y.V., Yardimci, H., Long, D.T., Ho, T.V., Guainazzi, A., Bermudez, V.P., Hurwitz, J., van Oijen, A., Schärer, O.D., and Walter, J.C. (2011). Selective bypass of a lagging strand roadblock by the eukaryotic replicative DNA helicase. Cell *146*, 931–941.

Garaycoechea, J.I., Crossan, G.P., Langevin, F., Daly, M., Arends, M.J., and Patel, K.J. (2012). Genotoxic consequences of endogenous aldehydes on mouse haematopoietic stem cell function. Nature *489*, 571–575.

Ghosal, G., Leung, J.W., Nair, B.C., Fong, K.W., and Chen, J. (2012). Proliferating cell nuclear antigen (PCNA)-binding protein C1orf124 is a regulator of translesion synthesis. J. Biol. Chem. *287*, 34225–34233.

Grogan, D., and Jinks-Robertson, S. (2012). Formaldehyde-induced mutagenesis in Saccharomyces cerevisiae: molecular properties and the roles of repair and bypass systems. Mutat. Res. *731*, 92–98.

Hoege, C., Pfander, B., Moldovan, G.L., Pyrowolakis, G., and Jentsch, S. (2002). RAD6-dependent DNA repair is linked to modification of PCNA by ubiquitin and SUMO. Nature *419*, 135–141.

Hoeijmakers, J.H.J. (2001). Genome maintenance mechanisms for preventing cancer. Nature *411*, 366–374.

Iyer, L.M., Koonin, E.V., and Aravind, L. (2004). Novel predicted peptidases with a potential role in the ubiquitin signaling pathway. Cell Cycle *3*, 1440–1450.

Jentsch, S., and Psakhye, I. (2013). Control of nuclear activities by substrate-selective and protein-group SUMOylation. Annu. Rev. Genet. *47*, 167–186.

Jentsch, S., and Rumpf, S. (2007). Cdc48 (p97): a "molecular gearbox" in the ubiquitin pathway? Trends Biochem. Sci. *32*, 6–11.

Juhasz, S., Balogh, D., Hajdu, I., Burkovics, P., Villamil, M.A., Zhuang, Z., and Haracska, L. (2012). Characterization of human Spartan/C1orf124, an ubiquitin-PCNA interacting regulator of DNA damage tolerance. Nucleic Acids Res. *40*, 10795–10808.

Kanellis, P., Gagliardi, M., Banath, J.P., Szilard, R.K., Nakada, S., Galicia, S., Sweeney, F.D., Cabelof, D.C., Olive, P.L., and Durocher, D. (2007). A screen for suppressors of gross chromosomal rearrangements identifies a conserved role for PLP in preventing DNA lesions. PLoS Genet. *3*, e134.

Kim, M.S., Machida, Y., Vashisht, A.A., Wohlschlegel, J.A., Pang, Y.P., and Machida, Y.J. (2013). Regulation of error-prone translesion synthesis by Spartan/C1orf124. Nucleic Acids Res. *41*, 1661–1668.

Kohn, K.W., Shao, R.G., and Pommier, Y. (2000). How do drug-induced topoisomerase I-DNA lesions signal to the molecular interaction network that regulates cell cycle checkpoints, DNA replication, and DNA repair? Cell Biochem. Biophys. *33*, 175–180.

Kooistra, S.M., and Helin, K. (2012). Molecular mechanisms and potential functions of histone demethylases. Nat. Rev. Mol. Cell Biol. *13*, 297–311.

Lambert, S., Watson, A., Sheedy, D.M., Martin, B., and Carr, A.M. (2005). Gross chromosomal rearrangements and elevated recombination at an inducible site-specific replication fork barrier. Cell *121*, 689–702.

Langevin, F., Crossan, G.P., Rosado, I.V., Arends, M.J., and Patel, K.J. (2011). Fancd2 counteracts the toxic effects of naturally produced aldehydes in mice. Nature *475*, 53–58.

Li, X., and Heyer, W.D. (2008). Homologous recombination in DNA repair and DNA damage tolerance. Cell Res. *18*, 99–113.

Lieber, M.R. (2010). The mechanism of double-strand DNA break repair by the nonhomologous DNA end-joining pathway. Annu. Rev. Biochem. *79*, 181–211.

Machida, Y., Kim, M.S., and Machida, Y.J. (2012). Spartan/C1orf124 is important to prevent UV-induced mutagenesis. Cell Cycle *11*, 3395–3402.

Mao, Y., Sun, M., Desai, S.D., and Liu, L.F. (2000). SUMO-1 conjugation to topoisomerase I: A possible repair response to topoisomerase-mediated DNA damage. Proc. Natl. Acad. Sci. USA *97*, 4046–4051.

Mieczkowski, P.A., Lemoine, F.J., and Petes, T.D. (2006). Recombination between retrotransposons as a source of chromosome rearrangements in the yeast Saccharomyces cerevisiae. DNA Repair (Amst.) *5*, 1010–1020.

Minko, I.G., Zou, Y., and Lloyd, R.S. (2002). Incision of DNA-protein crosslinks by UvrABC nuclease suggests a potential repair pathway involving nucleotide excision repair. Proc. Natl. Acad. Sci. USA *99*, 1905–1909.

Moldovan, G.L., and D'Andrea, A.D. (2009). How the fanconi anemia pathway guards the genome. Annu. Rev. Genet. *43*, 223–249.

Mosbech, A., Gibbs-Seymour, I., Kagias, K., Thorslund, T., Beli, P., Povlsen, L., Nielsen, S.V., Smedegaard, S., Sedgwick, G., Lukas, C., et al. (2012). DVC1 (C1orf124) is a DNA damage-targeting p97 adaptor that promotes ubiquitin-dependent responses to replication blocks. Nat. Struct. Mol. Biol. *19*, 1084–1092.

Mullen, J.R., Chen, C.F., and Brill, S.J. (2010). Wss1 is a SUMO-dependent isopeptidase that interacts genetically with the Slx5-Slx8 SUMO-targeted ubiquitin ligase. Mol. Cell. Biol. *30*, 3737–3748.

Mullen, J.R., Das, M., and Brill, S.J. (2011). Genetic evidence that polysumoylation bypasses the need for a SUMO-targeted Ub ligase. Genetics *187*, 73–87.

Nakano, T., Morishita, S., Katafuchi, A., Matsubara, M., Horikawa, Y., Terato, H., Salem, A.M., Izumi, S., Pack, S.P., Makino, K., and Ide, H. (2007). Nucleotide excision repair and homologous recombination systems commit differentially to the repair of DNA-protein crosslinks. Mol. Cell *28*, 147–158.

Nakano, T., Miyamoto-Matsubara, M., Shoulkamy, M.I., Salem, A.M., Pack, S.P., Ishimi, Y., and Ide, H. (2013). Translocation and stability of replicative DNA helicases upon encountering DNA-protein cross-links. J. Biol. Chem. *288*, 4649–4658.

Nie, M., Aslanian, A., Prudden, J., Heideker, J., Vashisht, A.A., Wohlschlegel, J.A., Yates, J.R., 3rd, and Boddy, M.N. (2012). Dual recruitment of Cdc48 (p97)-Ufd1-Npl4 ubiquitin-selective segregase by small ubiquitin-like modifier

protein (SUMO) and ubiquitin in SUMO-targeted ubiquitin ligase-mediated genome stability functions. J. Biol. Chem. *287*, 29610–29619.

Nouspikel, T. (2009). DNA repair in mammalian cells : Nucleotide excision repair: variations on versatility. Cell. Mol. Life Sci. *66*, 994–1009.

Pommier, Y., Barcelo, J.M., Rao, V.A., Sordet, O., Jobson, A.G., Thibaut, L., Miao, Z.H., Seiler, J.A., Zhang, H., Marchand, C., et al. (2006). Repair of Topoisomerase I-Mediated DNA Damage. Prog. Nucleic Acid Res. Mol. Biol. *81*, 179–229.

Pouliot, J.J., Yao, K.C., Robertson, C.A., and Nash, H.A. (1999). Yeast gene for a Tyr-DNA phosphodiesterase that repairs topoisomerase I complexes. Science *286*, 552–555.

Pourquier, P., Ueng, L.M., Kohlhagen, G., Mazumder, A., Gupta, M., Kohn, K.W., and Pommier, Y. (1997). Effects of uracil incorporation, DNA mismatches, and abasic sites on cleavage and religation activities of mammalian topoisomerase I. J. Biol. Chem. *272*, 7792–7796.

Psakhye, I., and Jentsch, S. (2012). Protein group modification and synergy in the SUMO pathway as exemplified in DNA repair. Cell *151*, 807–820.

Quievryn, G., and Zhitkovich, A. (2000). Loss of DNA-protein crosslinks from formaldehyde-exposed cells occurs through spontaneous hydrolysis and an active repair process linked to proteosome function. Carcinogenesis *21*, 1573–1580.

Regairaz, M., Zhang, Y.W., Fu, H., Agama, K.K., Tata, N., Agrawal, S., Aladjem, M.I., and Pommier, Y. (2011). Mus81-mediated DNA cleavage resolves replication forks stalled by topoisomerase I-DNA complexes. J. Cell Biol. *195*, 739–749.

Rosado, I.V., Langevin, F., Crossan, G.P., Takata, M., and Patel, K.J. (2011). Formaldehyde catabolism is essential in cells deficient for the Fanconi anemia DNA-repair pathway. Nat. Struct. Mol. Biol. *18*, 1432–1434.

Sale, J.E. (2013). Translesion DNA synthesis and mutagenesis in eukaryotes. Cold Spring Harb. Perspect. Biol. *5*, a012708.

Stapf, C., Cartwright, E., Bycroft, M., Hofmann, K., and Buchberger, A. (2011). The general definition of the p97/valosin-containing protein (VCP)-interacting motif (VIM) delineates a new family of p97 cofactors. J. Biol. Chem. *286*, 38670–38678.

Stolz, A., Hilt, W., Buchberger, A., and Wolf, D.H. (2011). Cdc48: a power machine in protein degradation. Trends Biochem. Sci. *36*, 515–523.

Su, D., and Hochstrasser, M. (2010). A WLM protein with SUMO-directed protease activity. Mol. Cell. Biol. *30*, 3734–3736.

Swenberg, J.A., Lu, K., Moeller, B.C., Gao, L., Upton, P.B., Nakamura, J., and Starr, T.B. (2011). Endogenous versus exogenous DNA adducts: their role in carcinogenesis, epidemiology, and risk assessment. Toxicol. Sci. *120* (*Suppl 1*), S130–S145.

Trewick, S.C., Henshaw, T.F., Hausinger, R.P., Lindahl, T., and Sedgwick, B. (2002). Oxidative demethylation by Escherichia coli AlkB directly reverts DNA base damage. Nature *419*, 174–178.

Vaz, B., Halder, S., and Ramadan, K. (2013). Role of p97/VCP (Cdc48) in genome stability. Front Genet. *4*, 60.

Zharkov, D.O. (2008). Base excision DNA repair. Cell. Mol. Life Sci. *65*, 1544–1565.